

# Second Order Statistics For Composite $\kappa$ - $\mu$ Fading Model

Rafael Augusto Pedriali, Elvio João Leonardo, and Michel Daoud Yacoub

**Abstract**—This paper considers second order statistics for the composite  $\kappa$ - $\mu$  fading model. More specifically, level crossing rate and average fade duration are calculated, and two formulations are offered: exact and approximate. The exact formulation is given in integral form, and the approximate one is written in terms of the Fox  $H$ -function, and also expressed as an infinite summation. The computation of the approximate level crossing rate and average fade duration converges quickly and are practically coincident with the exact solutions for the composite multipath-shadowing environment considered here. Additionally, as an application example, the cascaded fading channel is analyzed.

**Keywords**—level crossing rate, average fade duration, composite fading, cascaded fading channel.

## I. INTRODUCTION

In wireless communications, signal level variations are usually modeled according to the specific scenarios involved, with the goal of representing the signal distortion imposed by the channel. Such variations are caused by several factors, such as reflection, refraction, diffraction, Doppler frequency, shadowing and multipath effects. There are in the literature numerous methods which try to predict the signal level variation [1], with statistical models usually offering more accurate results. Currently, statistical models are divided into two classes, multipath (related to the short-term signal variation) and shadowing (related to the long-term signal variation). The first one deals with the fast fluctuation of the signal caused by scattering in urban and rural environments. A large number of distributions are used to model fast fading, such as Rayleigh, Nakagami- $m$ ,  $\kappa$ - $\mu$ ,  $\alpha$ - $\mu$ , and others, which are all special cases of the more general distribution, namely  $\alpha$ - $\eta$ - $\kappa$ - $\mu$  [2]. Shadowing is concerned with slow fluctuations of the signal, which is induced by large obstructions such as buildings and hills. Probably the most used model to represent slow fading is the Lognormal distribution. However, due to its difficult algebraic manipulation, other distributions can be used to approximate the slow fading channel [1]. Although the characterization of fading into separate fast and slow phenomena is widely used, recent advances consider the combined effects of both fadings, in what is termed composite fading models. This is particularly desirable in non-stationary environments, when the local mean may also fluctuate rapidly.

Rafael A. Pedriali and Michel D. Yacoub are with the Wireless Technology Laboratory, School of Electrical and Computer Engineering, University of Campinas, Brazil (e-mail: rafa.a.p@decom.fee.unicamp.br; michel@decom.fee.unicamp.br). Elvio J. Leonardo is with the Department of Informatics, State University of Maringá, Brazil (e-mail: ejleonardo@uem.br). This work was supported in part by CNPq under Grants 304248/2014-2 and 141425/2019-9.

Composite fading models can be constructed by the product of two distributions, each representing the intended fading phenomenon. In its turn, the product of random variables is a broadly investigated topic, and appears in several applications. For instance, the cascaded channel is a classic example of use of the product of random variables [3]. The cascaded channel is also employed to model RFID systems [4]. The keyhole effect in MIMO systems [5], the statistics of the multi-hop communication channel [6], and high resolution synthetic aperture radar clutter [7] can all be modeled by the product of the appropriate random variables. In addition, the analysis of composite fading models can be found in several papers, e.g., [8]–[11], usually concentrating only in first order statistics. In this paper, our interest lays with the level crossing rate (LCR) and the average fade duration (AFD), which are important metrics belonging to second order statistics, and have important information about how fading is related to time [1]. LCR and AFD can be used, for instance, in burst error statistics, which are useful in predicting the performance of various modulations and adaptive modulation schemes [12], or in the selection of error correction codes [13], and MIMO systems analysis [14], [15], and also in ultra-reliable low-latency communication [16]. These characteristics are useful for the best performance of 5G networks. An LCR framework for composite fading models was introduced in [17], and after that several papers have worked with second order statistics of composite fading channels, e.g., [18]–[22]. Further, the authors in [22] propose a new, simple, accurate, and general approximation for LCR in composite fading environments. In this article, we apply the results from [22] to analyze and solve the LCR for the composite  $\kappa$ - $\mu$  fading model, in which fast and slow fadings are modeled by the  $\kappa$ - $\mu$  distribution. Note that the slow fading model assumes lower Doppler shift, this way matching with the signal's slow fluctuation.

This article is organized as follows. Section II briefly reviews the required background information. Section III presents the LCR and AFD for composite  $\kappa$ - $\mu$  fading with some plots and their interpretations. In Section IV an application of the obtained formulations over a generic cascaded fading channel is explored, and Section IV concludes this article.

## II. FRAMEWORK

### A. Level Crossing Rate and Average Fade Duration

The LCR for envelope  $E$ , represented as  $N_E(e)$ , is statistically defined as the average number of times that a signal crosses a particular threshold in a positive or negative

direction, i.e.,

$$N_E(e) = \int_0^\infty \dot{e} f_{E,\dot{E}}(e = E, \dot{e}) d\dot{e}, \quad (1)$$

in which,  $f_{E,\dot{E}}(e, \dot{e})$  is the joint probability density function (PDF) of the envelope and its time derivative  $\dot{E}$ .

The AFD, represented as  $T_E(e)$ , is calculated by

$$T_E(e) = \frac{F_E(e)}{N_E(e)}, \quad (2)$$

in which  $F_E(e)$  is the cumulative distribution function (CDF) of the envelope. This metric corresponds to the average time that the signal remains below a particular threshold [1].

### B. Fading Model

The  $\kappa$ - $\mu$  fading model, introduced in [23], is better suited to represent the signal variation in the presence of dominant *line-of-sight* (LOS) components. The PDF of the envelope is given by

$$f_E(e) = \frac{2\mu(\kappa+1)^{\frac{\mu+1}{2}}}{\kappa^{\frac{\mu-1}{2}} \exp(\kappa\mu)} \left(\frac{e}{\hat{e}}\right)^\mu \exp\left[-\mu(\kappa+1)\left(\frac{e}{\hat{e}}\right)^2\right] \times I_{\mu-1}\left(2\mu\sqrt{\kappa(\kappa+1)}\frac{e}{\hat{e}}\right), \quad (3)$$

in which  $\hat{e} = \sqrt{\mathbb{E}(E^2)}$  is the root mean square (*rms*) value of  $E$ ,  $\kappa > 0$  is the ratio between the powers of the dominant components and the scattered waves,  $\mu$  represents the real extension of the number of multipath clusters,  $I_\nu(\cdot)$  is the modified Bessel function of the first kind and order  $\nu$  [24, Eq. 9.6.20], and  $\mathbb{E}(\cdot)$  is the expectation operator.

In addition, other required metrics of the  $\kappa$ - $\mu$  model used in this article are the joint PDF of the envelope and its time derivative, and the LCR. These expressions were obtained from [25] and are, respectively, given as

$$f_{E,\dot{E}}(e, \dot{e}) = \frac{2\mu(\kappa+1)^{\frac{\mu+1}{2}}}{\kappa^{\frac{\mu-1}{2}} \exp(\kappa\mu)} \left(\frac{e}{\hat{e}}\right)^\mu \exp\left[-\mu(\kappa+1)\left(\frac{e}{\hat{e}}\right)^2\right] \times I_{\mu-1}\left(2\mu\sqrt{\kappa(\kappa+1)}\frac{e}{\hat{e}}\right) \times \frac{\sqrt{\mu(\kappa+1)}}{\sqrt{2\pi^{3/2}\hat{e}f_d}} \exp\left[-\frac{\mu(\kappa+1)}{2\pi^2 f_d^2} \left(\frac{\dot{e}}{\hat{e}}\right)^2\right], \quad (4)$$

and

$$N_E(e) = \frac{\sqrt{2\pi\mu}f_d(\kappa+1)^{\frac{\mu}{2}}}{\kappa^{\frac{\mu-1}{2}} \exp(\kappa\mu)} \left(\frac{e}{\hat{e}}\right)^\mu \exp\left[-\mu(\kappa+1)\left(\frac{e}{\hat{e}}\right)^2\right] \times I_{\mu-1}\left(2\mu\sqrt{\kappa(\kappa+1)}\frac{e}{\hat{e}}\right), \quad (5)$$

in which  $f_d$  is the maximum Doppler shift.

### C. Composite Fading Statistics

The framework given in the following introduces the statistical formulations needed for the development of the proposed work. Let us consider a composite fading process whose envelope  $C$  is modeled by the product of two random variables (RVs) denominated  $S$  (as in short-term process) and  $L$  (as in long-term process), i.e.,

$$C = S \times L, \quad (6)$$

and its time derivative  $\dot{C}$  given by

$$\dot{C} = \dot{S} \times L + S \times \dot{L}, \quad (7)$$

in which  $\dot{S}$  and  $\dot{L}$  correspond to the time derivative of  $S$  and  $L$ , respectively. Also, considering this scenario, the PDF of the envelope  $C$  is defined by

$$f_C(c) = \int_0^\infty \frac{1}{l} f_S\left(\frac{c}{l}\right) f_L(l) dl, \quad (8)$$

in which  $f_S(s)$  and  $f_L(l)$  are the PDFs of RVs  $S$  and  $L$ , respectively.

If we assume that  $S$  and  $L$  are  $\kappa$ - $\mu$  distributed RVs, the CDF of  $C$  is calculated in [8], and is given in (12) at the top of the next page, in which  ${}_1F_1(\cdot)$  is the confluent hypergeometric function of the first kind [24, 13.1.2],  $\Gamma(\cdot)$  is the gamma function [24, 6.1.1], and  $\rho = \frac{c}{\hat{s}\hat{l}}$  is the normalized envelope.

Additionally, as shown in [22], after manipulating (6) and (7), the composite PDF of  $C$  and  $\dot{C}$  is given by

$$f_{C,\dot{C}}(c, \dot{c}) = \int_0^\infty \int_{-\infty}^\infty \frac{1}{l^2} f_{S,\dot{S}}\left(\frac{c}{l}, \frac{\dot{c}}{l} - \frac{\dot{l}c}{l^2}\right) f_{L,\dot{L}}(l, \dot{l}) d\dot{l} dl. \quad (9)$$

Following the development introduced in [22], the exact and approximate formulations for LCR, respectively, are given by

$$N_C(c) = \int_0^\infty \int_0^\infty \int_{-\infty}^\infty \frac{1}{l^2} f_{S,\dot{S}}\left(\frac{c}{l}, \frac{\dot{c}}{l} - \frac{\dot{l}c}{l^2}\right) f_{L,\dot{L}}(l, \dot{l}) d\dot{l} dl d\dot{c}, \quad (10)$$

$$N_C(c) \approx \int_0^\infty N_S\left(\frac{c}{l}\right) f_L(l) dl = \mathbb{E}_L\left(N_S\left(\frac{c}{l}\right)\right). \quad (11)$$

The approximate expression is obtained if one considers that  $\frac{\dot{l}c}{l^2}$  tends to zero in (10), which is expected for the proposed model in which the time scale of slow and fast fading are significantly different. Please refer to [22] for details.

### III. LCR AND AFD FOR COMPOSITE $\kappa$ - $\mu$ FADING CHANNEL

In this section, exact and approximate expressions for LCR and AFD assuming composite  $\kappa$ - $\mu$  fading model are obtained and compared. Furthermore, the results are given in terms of the normalized Doppler shift ratio  $f = \frac{\dot{L}}{f_S}$ .

The exact LCR for the composite  $\kappa$ - $\mu$  fading model is obtained by using (4) in (10), resulting in (13), given at the top of the next page. Note that the result is given in terms of an integral in  $u$ , which is obtained by changing the integration variable to  $l = u\hat{l}$ , since it is easier to integrate in  $\hat{l}$  and  $\dot{c}$  than in  $u$ . The approximate expression is obtained by using (3) and (5) in (11), resulting in (14) at the top of the next page, its demonstration is given in the Appendix.

The calculation of (14) converges rapidly, with just a few terms of the summation in most cases. In addition, an alternative expression for the approximate LCR for composite  $\kappa$ - $\mu$  fading was obtained, given in terms of the multivariate Fox  $H$ -function, which guarantees the convergence of the integral form [26]. This is expressed as

$$N_C(\rho) \approx \sqrt{2\pi} f_S \frac{[\rho^2(\kappa_L+1)\mu_L(\kappa_S+1)\mu_S]^{\mu_S-\frac{1}{2}}}{\exp(\kappa_L\mu_L + \kappa_S\mu_S)} \times H[X; (\alpha, \mathbf{A}); (\beta, \mathbf{B}); \mathcal{L}_S], \quad (15)$$

$$F_C(\rho) = \frac{1}{\Gamma(\mu_L)\Gamma(\mu_S)} \sum_{j=0}^{\infty} \frac{(-1)^j}{j!} \times \left\{ \frac{[\rho^2(\kappa_L+1)\mu_L(\kappa_S+1)\mu_S]^{j+\mu_S}}{j+\mu_S} {}_1F_1(j+\mu_S; \mu_S; -\kappa_S\mu_S) \Gamma(-j+\mu_L-\mu_S) {}_1F_1(j+\mu_S; \mu_L; -\kappa_L\mu_L) + \frac{[\rho^2(\kappa_L+1)\mu_L(\kappa_S+1)\mu_S]^{j+\mu_L}}{j+\mu_L} {}_1F_1(j+\mu_L; \mu_L; -\kappa_L\mu_L) \Gamma(-j-\mu_L+\mu_S) {}_1F_1(j+\mu_L; \mu_S; -\kappa_S\mu_S) \right\} \quad (12)$$

$$N_C(\rho) = \frac{2f_S \sqrt{2\pi\kappa_L\mu_L\kappa_S\mu_S}}{\exp(\kappa_L\mu_L + \kappa_S\mu_S)} \left(\frac{\kappa_L+1}{\kappa_L}\right)^{\frac{\mu_L}{2}} \left(\frac{\kappa_S+1}{\kappa_S}\right)^{\frac{\mu_S}{2}} \int_0^{\infty} \rho^{\mu_S} u^{\mu_L-\mu_S-2} \sqrt{f^2\rho^2(\kappa_S+1)\mu_S + u^4(\kappa_L+1)\mu_L} \times \exp\left[-u^2(\kappa_L+1)\mu_L - \frac{\rho^2(\kappa_S+1)\mu_S}{u^2}\right] I_{\mu_L-1}\left(2u\sqrt{\kappa_L(\kappa_L+1)\mu_L}\right) I_{\mu_S-1}\left(\frac{2\rho\sqrt{\kappa_S(\kappa_S+1)\mu_S}}{u}\right) du \quad (13)$$

$$N_C(\rho) \approx \frac{1}{\Gamma(\mu_L)\Gamma(\mu_S)} \frac{\sqrt{2\pi}f_S}{\exp(\kappa_L\mu_L + \kappa_S\mu_S)} \sum_{j=0}^{\infty} \frac{(-1)^j}{j!} \times \left\{ [\rho^2(\kappa_L+1)\mu_L(\kappa_S+1)\mu_S]^{j+\mu_S-\frac{1}{2}} {}_1F_1(-j; \mu_S; \kappa_S\mu_S) \Gamma\left(-j+\mu_L-\mu_S+\frac{1}{2}\right) {}_1F_1\left(-j+\mu_L-\mu_S+\frac{1}{2}; \mu_L; \kappa_L\mu_L\right) + [\rho^2(\kappa_L+1)\mu_L(\kappa_S+1)\mu_S]^{j+\mu_L} {}_1F_1(-j; \mu_L; \kappa_L\mu_L) \Gamma\left(-j-\mu_L+\mu_S-\frac{1}{2}\right) {}_1F_1\left(-j-\mu_L+\mu_S-\frac{1}{2}; \mu_S; \kappa_S\mu_S\right) \right\} \quad (14)$$

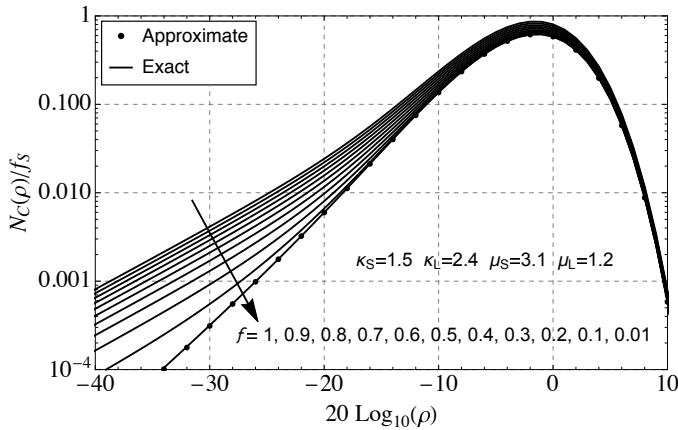


Fig. 1. Comparison between the exact (lines) and approximate (dots) LCR for composite  $\kappa$ - $\mu$  distribution with fixed  $\kappa_S = 1.5$ ,  $\kappa_L = 2.4$ ,  $\mu_S = 3.1$ ,  $\mu_L = 1.2$  and with different values of  $f$ .

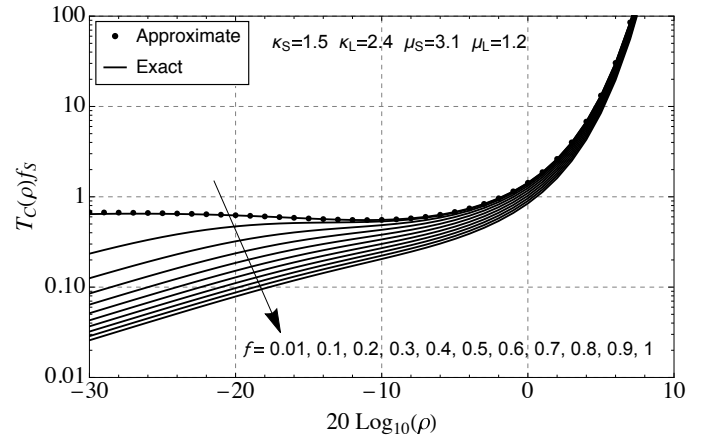


Fig. 2. Comparison between the exact (lines) and approximate (dots) AFD for composite  $\kappa$ - $\mu$  distribution with fixed  $\kappa_S = 1.5$ ,  $\kappa_L = 2.4$ ,  $\mu_S = 3.1$ ,  $\mu_L = 1.2$  and with different values of  $f$ .

in which  $\mathcal{L}_S$  is the appropriate contour on the complex plane  $\mathbf{S}$ , with  $\mathbf{S} = [S_1, S_2, S_3]$ , and

$$X = \begin{bmatrix} \rho^2(\kappa_L+1)\mu_L(\kappa_S+1)\mu_S, -\kappa_L\mu_L, \\ -\rho^2(\kappa_L+1)\mu_L\kappa_S(\kappa_S+1)\mu_S^2 \end{bmatrix},$$

$$\alpha = \left[ 0, 0, 0, \mu_L - \mu_S + \frac{1}{2} \right], \quad \beta = [\mu_L, \mu_S],$$

$$\mathbf{A} = \begin{bmatrix} 1 & 0 & 0 \\ 0 & 1 & 0 \\ 0 & 0 & 1 \\ 1 & -1 & 1 \end{bmatrix}, \quad \text{and} \quad \mathbf{B} = \begin{bmatrix} 0 & -1 & 0 \\ 0 & 0 & -1 \end{bmatrix}. \quad (16)$$

Details of the development of this formulation are also given in the Appendix.

It can be observed that the exact and approximate formulations depend on  $\rho$  and  $f_S$ . The variable  $f_L$  appears only in the exact formulation but in the form of the ratio  $f_L/f_S$ , i.e., the normalized Doppler shift ratio. Another important

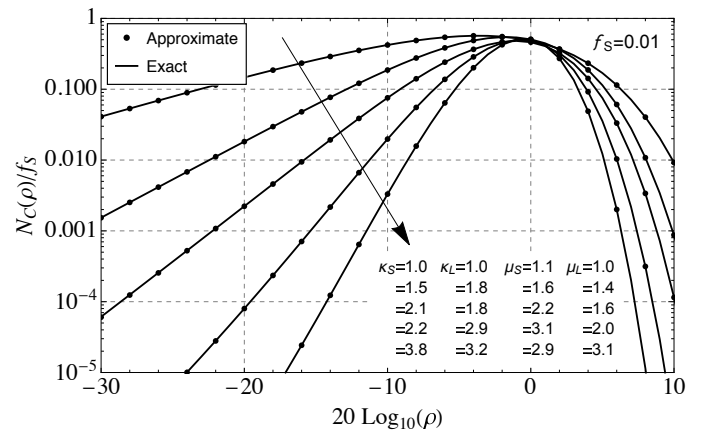


Fig. 3. Comparison between the exact (lines) and approximate (dots) LCR for composite  $\kappa$ - $\mu$  distribution with different values of  $\kappa_S$ ,  $\kappa_L$ ,  $\mu_S$ ,  $\mu_L$  and a fixed  $f = 0.01$ .

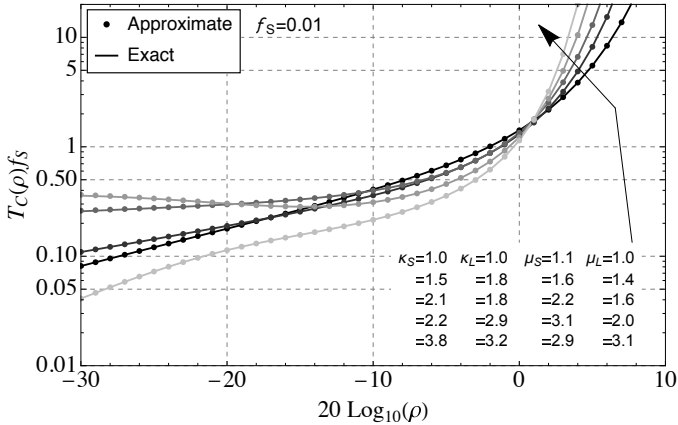


Fig. 4. Comparison between the exact (lines) and approximate (dots) AFD for composite  $\kappa$ - $\mu$  distribution with different values of  $\kappa_S$ ,  $\kappa_L$ ,  $\mu_S$ ,  $\mu_L$  and a fixed  $f = 0.01$ .

point that can be observed is that, for second order statistics in composite fading models, swapping the position of the individual distributions alters the final result, which can be easily checked in (13) and (14). This is not observed in first order statistics, when swapping the order of the distributions does not change the results, as presented in [8]. The AFD for the proposed composite fading model is obtained by using the CDF (12) in (2).

Figs. 1 and 2 show results for the exact (solid lines) and approximate (dots) LCR and AFD plots, with fixed  $\kappa$ - $\mu$  fading parameters and different values for  $f$ . Note that, for lower values of the ratio  $f$ , the approximate and exact curves are indistinguishable. This happens because for lower values of  $f$  the approximation tends to the exact solution. Furthermore, if  $f$  increases, then the assumption considered for the approximation fails and the difference between the results also increases. However, in practical cases the signal variation rate of a shadowing process is much slower than the multipath one. In this sense, it is convenient to claim  $f \ll 1$  and the approximate solution is perfectly suitable to assess LCR in composite multipath-shadowing environments.

Figs. 3 and 4 compares the exact and approximate curves for LCR and AFD for practical cases, with fixed  $f = 0.01$ , and different fading parameters. Similarly to the above comments, and independently of physical parameters values, if  $f$  has a small value (as in this case), then the exact and approximate results are practically coincident, as shown in the figures.

#### IV. CASCADED FADING CHANNEL

In a cascaded fading channel, the source and destination terminals communicate with each other through relay terminals or keyholes effect, which are viewed as a channel modeled by product of random variables. In both cases, the instantaneous signal to noise ratio (SNR) at the destination terminal is expressed by [3],

$$\gamma = \frac{E_s}{N_t} \prod_{n=1}^N (R_n)^2 \quad (17)$$

in which  $R_n$  is the wireless channel gain,  $N$  is the number of relay terminals or keyholes in the system,  $E_s$  is the average

energy of the transmitted symbols, and  $N_t$  is the noise power spectral density.

As an example, suppose a cascaded fading channel composed by two-tap relay or keyhole, which is modeled by the product between two random variables ( $S$  and  $L$ ), both following the  $\kappa$ - $\mu$  distribution. In this case, the instantaneous SNR is

$$\gamma = \frac{E_s}{N_t} (SL)^2 = \frac{E_s}{N_t} C^2. \quad (18)$$

Therefore, the LCR and AFD for the instantaneous SNR in this system is given, respectively, by

$$N_\gamma(\gamma) = N_C \left( \sqrt{\gamma \frac{N_t}{E_s}} \right) \quad (19)$$

and

$$T_\gamma(\gamma) = T_C \left( \sqrt{\gamma \frac{N_t}{E_s}} \right). \quad (20)$$

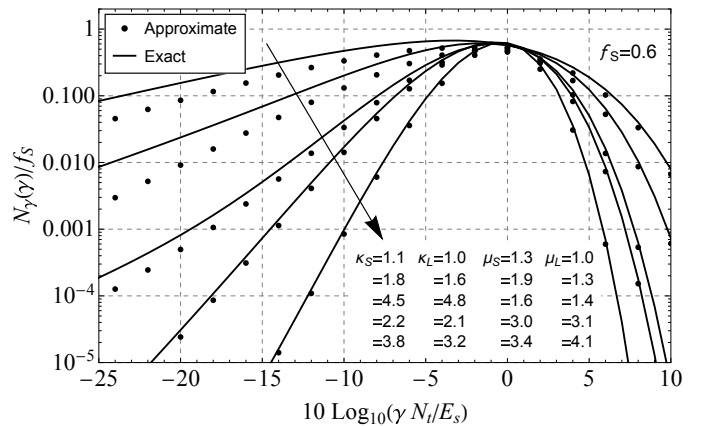


Fig. 5. Level crossing rate application for a generic cascaded fading channel following a composite  $\kappa$ - $\mu$  model.

The plots in Fig. 5 are obtained using (19), (13), and (14), and are normalized by the cascaded system variables  $E_s$  and  $N_t$ . Additionally, the figure compares the exact (lines) and approximate (dots) LCR curves with different fading parameters and using  $f = 0.6$ . It can be observed that the approximate formulation produces good results for higher fading parameters values, even considering higher  $f$  values.

#### V. CONCLUSION

In this article, LCR and AFD results for the composite  $\kappa$ - $\mu$  fading model are formulated, and exact and approximate expressions are presented. Also, an application example considering this generic fading model is included. For the considered composite multipath-shadowing environment and assumptions given, approximate and exact results are indistinguishable from each other. In addition, the obtained formulations can be used in the analysis of digital communication systems for which the proposed composite fading model is assumed, allowing the interested reader to obtain several performance metrics.

#### ACKNOWLEDGMENT

This work was supported in part by CNPq under Grants 304248/2014-2 and 141425/2019-9.

## APPENDIX

Proof of the approximate LCR in (14) and (15).

- 1) Use (3) and (5) in (11), and also change the integration variable to  $l = \hat{l}u$ ;
- 2) Use [27, 01.03.07.0001.01], i.e.,  $e^z = \frac{1}{2\pi i} \oint_{\mathcal{L}_S} \Gamma(S)(-z)^{-S} dS$  and [27, 03.02.26.0008.01], i.e.,  $I_\nu(z) = \left(\frac{z}{2}\right)^\nu \frac{1}{2\pi i} \oint_{\mathcal{L}_S} \frac{\Gamma(S)}{\Gamma(-S+\nu+1)} \left(-\frac{z^2}{4}\right)^{-S} dS$ , to expand the exponential and Bessel functions, respectively, to contour integrals, in which  $i$  is the imaginary unit;
- 3) Use [28, 3.326.2] as the integration identity, to obtain

$$\begin{aligned}
 N_C(\rho) &\approx \sqrt{2\pi} f_S \frac{[\rho^2 (\kappa_L + 1) \mu_L (\kappa_S + 1) \mu_S]^{m_S - \frac{1}{2}}}{\exp(\kappa_L \mu_L + \kappa_S \mu_S)} \\
 &\times \left(\frac{1}{2\pi i}\right)^3 \oint \oint \oint_{\mathcal{L}_S} \frac{\Gamma(\mu_L - \mu_S + S_1 - S_2 + S_3 + \frac{1}{2})}{\Gamma(\mu_S - S_3)(\mu_L - S_2)} \\
 &\times [\rho^2 (\kappa_L + 1) \mu_L (\kappa_S + 1) \mu_S]^{-S_1} (-\kappa_L \mu_L)^{-S_2} \\
 &\times [-\rho^2 (\kappa_L + 1) \mu_L \kappa_S (\kappa_S + 1) \mu_S^2]^{-S_3} \\
 &\times \Gamma(S_1) \Gamma(S_2) \Gamma(S_3) dS_1 dS_2 dS_3. \quad (21)
 \end{aligned}$$

This expression can be written in terms of the Fox  $H$ -function, as presented in (15);

- 4) Use the residue theorem in (21) with the appropriate poles to find the expression in infinite summation as

$$\begin{aligned}
 N_C(\rho) &\approx \frac{\sqrt{2\pi} f_S}{\exp(\kappa_L \mu_L + \kappa_S \mu_S)} \sum_{k=0}^{\infty} \sum_{j=0}^{\infty} \sum_{i=0}^{\infty} \\
 &\times \frac{(-1)^{i+j} (-\kappa_L \mu_L)^j (\kappa_S \mu_S)^k}{i! j! k! \Gamma(j + \mu_L) (k + \mu_S)} \\
 &\times \left\{ [\rho^2 (\kappa_L + 1) \mu_L (\kappa_S + 1) \mu_S]^{i+k+\mu_S - \frac{1}{2}} \right. \\
 &\quad \times \Gamma\left(-i + j - k + \mu_L - \mu_S + \frac{1}{2}\right) \\
 &\quad + [\rho^2 (\kappa_L + 1) \mu_L (\kappa_S + 1) \mu_S]^{i+j+\mu_L} \\
 &\quad \left. \times \Gamma\left(-i - j + k - \mu_L + \mu_S - \frac{1}{2}\right) \right\}. \quad (22)
 \end{aligned}$$

After some algebraic manipulations, two of the summations are simplified and (14) is attained.

## REFERENCES

- [1] J. D. Parsons, *The mobile radio propagation channel*. Wiley, 2000.
- [2] M. D. Yacoub, "The  $\alpha - \eta - \kappa - \mu$  fading model," *IEEE Transactions on Antennas and Propagation*, vol. 64, no. 8, pp. 3597–3610, 2016.
- [3] F. Yilmaz and M. Alouini, "Product of the powers of generalized nakagami-m variates and performance of cascaded fading channels," in *Proc. 2009 IEEE Global Commun. Conf. (GLOBECOM)*, November 2009, pp. 1–8.
- [4] A. A. Farid and S. Hranilovic, "Outage capacity optimization for free-space optical links with pointing errors," *J. Lightwave Technol.*, vol. 25, no. 7, pp. 1702–1710, July 2007.
- [5] Y. Wu, G. Zheng, and T. Wang, "Performance analysis of mimo transmission scheme using single leaky coaxial cable," *IEEE Antennas Wireless Propag. Lett.*, vol. 16, pp. 298–301, May 2017.
- [6] M. F. Feteiha and M. H. Ahmed, "Multihop best-relay selection for vehicular communication over highways traffic," *IEEE Trans. on Veh. Technol.*, vol. 67, no. 10, pp. 9845–9855, October 2018.
- [7] K. D. Ward, C. J. Baker, and S. Watts, "Maritime surveillance radar. i. radar scattering from the ocean surface," *IEE Proc. F Radar and Signal Processing*, vol. 137, no. 2, pp. 51–62, April 1990.
- [8] C. R. N. da Silva, E. J. Leonardo, and M. D. Yacoub, "Product of two envelopes taken from  $\alpha$ - $\mu$ ,  $\kappa$ - $\mu$ , and  $\eta$ - $\mu$  distributions," *IEEE Transactions on Communications*, vol. 66, no. 3, pp. 1284–1295, March 2018.
- [9] E. J. Leonardo and M. D. Yacoub, "The product of two  $\alpha$ - $\mu$  variates and the composite  $\alpha$ - $\mu$  multipath-shadowing model," *IEEE Transactions on Vehicular Technology*, vol. 64, no. 6, pp. 2720–2725, June 2015.
- [10] A. A. Hammadi, O. Alhussein, P. C. Sofotasios, S. Muhaidat, M. Al-Qutayri, S. Al-Araji, G. K. Karagiannidis, and J. Liang, "Unified analysis of cooperative spectrum sensing over composite and generalized fading channels," *IEEE Transactions on Vehicular Technology*, vol. 65, no. 9, pp. 6949–6961, September 2016.
- [11] S. K. Yoo, S. L. Cotton, P. C. Sofotasios, M. Matthaiou, M. Valkama, and G. K. Karagiannidis, "The fisher–snedecor  $\mathcal{F}$  distribution: A simple and accurate composite fading model," *IEEE Communications Letters*, vol. 21, no. 7, pp. 1661–1664, July 2017.
- [12] J. M. Morris and J. Chang, "Burst error statistics of simulated viterbi decoded bfsk and high-rate punctured codes on fading and scintillating channels," *IEEE Transactions on Communications*, vol. 43, no. 2/3/4, pp. 694–700, February 1995.
- [13] M. Simon and M. Alouini, *Digital Communication over Fading Channels*, ser. Wiley Series in Telecommunications and Signal Processing. Wiley, 2005.
- [14] N. Zlatanov, Z. Hadzi-Velkov, and G. K. Karagiannidis, "Level crossing rate and average fade duration of the double nakagami-m random process and application in mimo keyhole fading channels," *IEEE Communications Letters*, vol. 12, no. 11, pp. 822–824, November 2008.
- [15] A. Abdi, C. Gao, and A. M. Haimovich, "Level crossing rate and average fade duration in mimo mobile fading channels," in *2003 IEEE 58th Vehicular Technology Conference. VTC 2003-Fall*, vol. 5, October 2003, pp. 3164–3168.
- [16] J. J. Nielsen, R. Liu, and P. Popovski, "Ultra-reliable low latency communication using interface diversity," *IEEE Transactions on Communications*, vol. 66, no. 3, pp. 1322–1334, March 2018.
- [17] A. Krantzik and D. Wolf, "Distribution of the fading-intervals of modified Suzuki processes," in *Proc. 5th European Signal Processing Conference*, vol. 1, 1990, pp. 361–364.
- [18] I. Trigui, A. Laourine, S. Affes, and A. Stephenne, "On the level crossing rate and average fade duration of composite multipath/shadowing channels," in *Global Communications Conference, 2008. (GLOBECOM 2008)*, November 2008, pp. 1–5.
- [19] P. Karadimas and S. A. Kotsopoulos, "The weibull–lognormal fading channel: Analysis, simulation, and validation," *IEEE Transactions on Vehicular Technology*, vol. 58, no. 7, pp. 3808–3813, July 2009.
- [20] J. Zhang, X. Chen, K. P. Peppas, X. Li, and Y. Liu, "On high-order capacity statistics of spectrum aggregation systems over  $\kappa$ - $\mu$  and  $\kappa$ - $\mu$  shadowed fading channels," *IEEE Transactions on Communications*, vol. 65, no. 2, pp. 935–944, February 2017.
- [21] S. K. Yoo, S. L. Cotton, P. C. Sofotasios, S. Muhaidat, and G. K. Karagiannidis, "Level crossing rate and average fade duration in  $\mathcal{F}$  composite fading channels," *IEEE Wireless Communications Letters*, vol. 9, no. 3, pp. 281–284, March 2020.
- [22] R. A. Pedriali, E. J. Leonardo, and M. D. Yacoub, "Higher order statistics for composite fading models," *IEEE Wireless Communications Letters*, vol. 8, no. 5, pp. 1493–1497, October 2019.
- [23] M. D. Yacoub, "The  $\kappa - \mu$  distribution and the  $\eta - \mu$  distribution," *IEEE Antennas Propag. Mag.*, vol. 49, no. 1, pp. 68–81, February 2007.
- [24] M. Abramowitz and I. A. Stegun, *Handbook of mathematical functions with formulas, graphs, and mathematical tables*, ser. A Wiley-Interscience publication. Wiley, 1972.
- [25] S. L. Cotton and W. G. Scanlon, "Higher-order statistics for  $\kappa - \mu$  distribution," *Electronics Letters*, vol. 43, no. 22, pp. 8715 – 8720, October 2007.
- [26] N. Hai and H. Srivastava, "The convergence problem of certain multiple mellin-barnes contour integrals representing h-functions in several variables," *Computers & Mathematics with Applications*, vol. 29, no. 6, pp. 17–25, March 1995.
- [27] Wolfram Research, Inc. (2020), *Wolfram Research*, Accessed: March 2019. [Online]. Available: <http://functions.wolfram.com>
- [28] A. Jeffrey and D. Zwillinger, *Table of Integrals, Series, and Products*. Elsevier Science, 2007.